CircRNA-associated ceRNA network reveals ErbB and Hippo signaling pathways in hypopharyngeal cancer

CHUN FENG[1], YUXIAO LI[1], YAN LIN[1], XIANBAO CAO[2], DONGDONG LI[3], HONGLEI ZHANG[4] and XIAOGUANG HE[1]

[1]The Second Department of Otolaryngology, Head and Neck Surgery of The First Affiliated Hospital of Kunming Medical University, Kunming, Yunnan 650223; [2]Department of Otolaryngology Head and Neck Surgery, Chinese PLA Kunming General Hospital, Kunming, Yunnan 650118; [3]Anhui Medical University, Hefei, Anhui 230022; [4]State Key Laboratory of Genetic Resources and Evolution, Kunming Institute of Zoology, Chinese Academy of Sciences, Kunming, Yunnan 650223, P.R. China

Received April 11, 2018; Accepted October 12, 2018

DOI: 10.3892/ijmm.2018.3942

Abstract. Accumulating evidence has suggested that circular RNAs (circRNAs), a novel class of non-coding RNAs, have crucial roles in tumor progression. However, the significance of circRNAs in hypopharyngeal cancer (HCa) remains to be investigated. The present study has identified aberrantly expressed circRNAs by performing circRNA sequencing analyses of three pairs of tumor and adjacent normal samples from patients with HCa. The results demonstrated that 173 circRNAs were differentially expressed (DE), including 71 upregulated and 102 downregulated circRNAs (FDR<0.05 and fold changes of ≥2 or ≤0.5 by Mann-Whitney U test followed by Benjamini-Hochberg correction for multiple testing). Pathway analyses of the genes producing DE circRNAs revealed that many of them were involved in cancer-related pathways. To further illustrate the roles of circRNAs in HCa progression, a competing endogenous RNA (ceRNAs) network was constructed, consisting of circRNAs, miRNA, and miRNA targeted genes. The results demonstrated that multiple cancer-related pathways were affected by performing enrichment analyses of the targeted genes. Of note, a ceRNA subnetwork was isolated, consisting of two circRNAs (hsa_circ_0008287 and hsa_circ_0005027) and one miRNA (hsa-miR-548c-3p), which significantly affect both ErbB and Hippo signaling pathways. In conclusion, the present study identified a set of circRNAs that are potentially implicated in the tumorigenesis of HCa and may serve as potential biomarkers for the diagnosis of HCa.

Correspondence to: Dr Xiaoguang He, The Second Department of Otolaryngology Head and Neck Surgery of The First Affiliated Hospital of Kunming Medical University, 295 Xichang Road, Kunming, Yunnan 650223, P.R. China
E-mail: hxiaoguang@163.com

Dr Honglei Zhang, State Key Laboratory of Genetic Resources and Evolution, Kunming Institute of Zoology, Chinese Academy of Sciences, 32 Jiaochang Donglu, Kunming, Yunnan 650223, P.R. China
E-mail: hlzhang2014@163.com

Abbreviations: HCa, hypopharyngeal cancer; DE, differentially expressed; ceRNAs, competing endogenous RNA; RPM, reads per Million mapped reads; GO, gene ontology; KEGG, Kyoto Encyclopedia of Genes and Genomes; PCA, principal component analysis

Key words: hypopharyngeal cancer, circular RNA, sequencing, epidermal growth factor receptor signaling pathway, Hippo signaling pathway, competing endogenous RNA network

Introduction

Hypopharyngeal carcinoma is a primary malignant tumor of the hypopharynx, accounting for 3-5% of the malignancies in the upper aerodigestive tract. Early diagnosis of hypopharyngeal cancer is hard because the early stages of hypopharyngeal carcinoma have no specific symptoms. Studies have reported that 60-80% of these patients had ipsilateral lymph node metastases and ≤40% of these patients have contralateral occult lymph node tumor deposits (1-3). Thus, the majority of patients with hypopharyngeal cancer have a poor prognosis and low survival rate (4). Therefore, identifying early stage indicators or biomarkers to improve patient survival is urgent.

Unlike normal linear RNA, the 3' and 5' ends of circular RNAs (circRNAs) are linked by covalent bonds and lack polarities or polyadenylated tails, thereby rendering them stable in tissues, serum and urine (5). Owing to this characteristic, the potential of circRNAs as biomarkers for human cancer has attracted significant focus. In addition, circRNAs are widely involved in cancer; ciRS-7 in HeLa cells (6), Hsa_circ_001569 in colorectal cancer (7), circHIPK3 in several types of cancer (8), f-circM9, f-circPR in hematological malignancy (9), and circTCF25 in urinary bladder carcinoma (10). Previous studies have demonstrated that the main function of circRNAs is that they can function as a microRNA (miRNA) sponge, binding to miRNAs and regulating them and their

downstream gene targets, through a competing endogenous (ce) RNA mechanism (11).

The present study comprehensively investigated the expression profile of circRNAs in HCa patients. The results identified a circRNA signature in HCa and suggested that a core miRNA-ceRNA network, regulating both the ErbB and Hippo signaling pathways, may have important roles in HCa progression.

Materials and methods

Patients and specimens. The study included three patients with HCa who underwent partial or radical cystectomies at the First Affiliated Hospital of Kunming Medical University (Kunming, China); samples were collected from March 2017 to October 2017. All three patients were male and their ages were 44, 54 and 56. Following surgery, the matched specimens were immediately preserved in liquid nitrogen until use. All patient samples were confirmed by pathological examination and none of the patients received neoadjuvant therapy. The study was approved by the Second Department of Otolaryngology Head and Neck Surgery of the First Affiliated Hospital of Kunming Medical University (Kunming, China). Written informed consent was obtained from all the participants in the study.

Total RNA isolation and quality control. Total RNA was isolated from samples using TRIzol reagent (Thermo Fisher Scientific, Inc., Waltham, MA, USA) following the manufacturer's protocol. The quantity and quality of total RNA samples were measured using NanoDrop ND-1000 (Thermo Fisher Scientific, Inc.). RNA integrity was assessed and confirmed via electrophoresis using denaturing agarose gels. Isolated RNA samples were stored at -80˚C prior to use.

Library preparation and sequencing. Total RNA from three matched HCa samples and adjacent normal tissues were treated with Epicenter Ribo-Zero rRNA Removal kit (Illumina, Inc., San Diego, CA, USA) and RNase R (Epicenter; Illumina, Inc.) to remove ribosomal and linear RNA. Then, the RNA-seq libraries were constructed using TruSeq Stranded Total RNA HT/LT Sample Prep kit (Illumina, Inc.). Sequencing was determined on Illumina Hiseq 2500 instrument with 2x150 bp paired reads.

Computational analysis of circRNAs. The clean reads were obtained after the raw reads were preprocessed with the FastQC quality control tool (12). CircRNAs were identified using CIRI (v.1.2) pipeline with default parameters (13). Genomic circRNAs were mapped to the human reference genome (GRCh37) by BWA (14). All circRNAs were annotated for circRNA-hosting genes with the application of GENCODE v24 (15). The identified circRNAs were converted to circRNA ID with web server circBase (16).

Principal component analysis (PCA). PCA was performed as previously described (17). A total of 4,634 distinct circRNAs with non-zero raw counts across the six samples were isolated and expressions of circRNAs were normalized with the reads per Million mapped reads (RPM) method and the expression matrix (each row represented a gene, each column represented a sample) were used for PCA. The prcomp package from R was used to perform PCA and the default parameters were used (18). The ggplot2 package from R was used to draw the scatter plot (19).

Normalization and differential expression analysis of circRNAs. Two steps were performed to normalize circRNA expression for depth. Firstly, the total back-spliced reads in a sample were counted and that number was divided by 1,000,000. This resulted in the 'per million' scaling factor. Secondly, the read counts were divided by the 'per million' scaling factor. This method normalized for sequencing depth, giving RPM. CircRNAs were isolated with RPM>0 across 6 samples and Mann-Whitney U test (20) (paired=T) followed by Benjamini-Hochberg multiple testing correction (21) were applied to identify the differentially expressed (DE) circRNAs. FDR<0.05 and a fold change of >2.0 or <0.5 were the selection criteria for significant DE circRNAs.

Functional enrichment analysis. Gene ontology (GO) term enrichment analysis and Kyoto Encyclopedia of Genes and Genomes (KEGG) pathway enrichment analysis were conducted with web server DAVID 6.8 (22). P<0.05 was considered as statistically significant.

CeRNA network. The top 20 upregulated circRNAs and the top 20 downregulated circRNAs were used to survey miRNA targets with the web tool CircInteractome (23). Specifically, CircInteractome downloads the mature sequences of circRNAs from the UCSC browser mirror (http://genome.mdc-berlin.de) (24) and predicts miRNAs that target circRNA by surveying for 7-mer or 8-mer complementarity to the seed region, as well as the 3'end of each miRNA using the TargetScan algorithm (25). The complete miRNA list and sequences were taken from the miRBase (http://www.mirbase.org/) (16). miRNA downstream targets were isolated with mirPath 3.0 (26) which was also used for miRNA KEGG pathway analysis. The ceRNA network was displayed by Cytoscape (v3.5.1) (27).

Reverse transcription-quantitative polymerase chain reaction (RT-qPCR). Total RNA was extracted from pooled normal and tumor tissue samples using TRIzol (Thermo Fisher Scientific, Inc.), and 1 μg of total RNA was reverse transcribed into first-strand cDNA using a PrimeScript RT Reagent kit (Takara Bio, Inc., Otsu, Japan), according to the manufacturer's protocols. qPCR was performed with a SYBR-Green real-time PCR kit (Thermo Fisher Scientific, Inc.) using the ABI StepOnePlus Real-Time PCR system (Applied Biosystems; Thermo Fisher Scientific, Inc.). CircRNAs were analyzed with 18s rRNA as the internal standard and miRNA was analyzed with U6 as the internal standard. The reactions were prepared as follows: 7.5 μl SYBR Premixm Ex Taq II, 0.25 μl ROX Reference Dye II, 0.125 μl forward primer, 0.125 μl reverse primer, 5 μl RNase-free water, and 2 μl cDNA. The thermocycling conditions were: one step at 95˚C for 30 sec, followed by 40 cycles of 95˚C for 5 sec and 60˚C for 30 sec, and a final step of 95˚C for 15 sec, 60˚C for 15 sec and 95˚C for 15 sec. Primer sequences are listed in Table I; expression levels were quantified via the $2^{-\Delta\Delta Cq}$ method (28).

Table I. Primer sequences used for reverse transcription-quantitative polymerase chain reaction analysis.

Gene	Forward primer (5'-3')	Reverse primer (5'-3')
hsa_circ_0004670	GCTCCCAAGCAAAAGAGAAG	CTGCTTTGTGCTTCCGTATTC
hsa_circ_0005703	TGGAGGAGAGGATCGAGTTC	GTTCTGGATGGTCTGCTTGG
hsa_circ_0003214	TGTGTTTGGAACTGCTACCG	ATCAGCCAGGGCACTCAATA
hsa_circ_0003146	CAACGACCTGGTGAAGAGG	GTCCGAGATCTCCAGCTTGT
hsa_circ_0002059	GCCGAGTTAATGGTGGGTTT	ACCAAATTCAGCCAGAATGC
hsa_circ_0002617	TTCCCCAGGAGTGTCAAGAT	TGGCAAAGATGAAAAGCTGA
hsa_circ_0000660	CTTCCAGTGGGAATCCACAT	AGACATTCTTCCCTTCCAACAA
hsa_circ_0054309	CTCTCAGCATGGGACCTTTT	CGATTTGGTTCTCCCATATCA
hsa_circ_0003279	CTCTGTGCACGACTCTCAGG	TCCCTTCTTCGCTCTTCTCA
hsa_circ_0000239	GAATGTTCAAATTGCTGCCATA	CCAGCAGCCCAACAATTACT
hsa_circ_0091382	CTGCAGGGTCTGTTTTTACCA	CCCATCCAGATCAAGAGAGC
hsa_circ_0004811	GGATCCAAAGGCACGTTTTA	AGAACTTCAGGCGCCAAGTA
hsa_circ_0007480	GTTGGAGGAAGGGAAAGAGC	ATGGCCACATCCCTAAATGT
hsa_circ_0013084	GGATGCTGCAAAAACGAGA	TGGGTTGTTTATACGACTTGGA
hsa_circ_0008836	CCTTTTGAGCTGGGAAAACT	TCTGAAGGAATTCGGGACAG
hsa_circ_0059060	GTGGAAGTGGAGAACCCAGA	ATGGGATGCTAGCCTTGAGA
hsa_circ_0001312	TCAGTACTCTGGGGGAAAGG	GCTGGGACAGATGAAACCAT
hsa_circ_0005027	TGTTGAGTTCGGCAGCATAC	ACACACCTCTGCAACCACAA
hsa_circ_0008287	CCGAGCCACCTAAACAACAG	TCTGGGAGCGTCAGAAAGTT
has-miR-548c-3p	CATTGGCATCTATTAGGTTG	GTATTAAGTTGGTGCAAAAG
18s rRNA	ACCTGGTTGATCCTGCCAG	TCCAAGTAGGAGAGGAGCG
U6	GTGCTCGCTTCGGCAGCA	TGGAACGCTTCACGAATTTG

Expression analysis of miR-548c-3p. Two methods were used to investigate the expression of miR-548c-3p among normal and tumor samples. The first was RT-qPCR, as detailed above. The second was in-silico analysis. The miRNA dataset of the esophageal carcinoma cohort from The Cancer Genome Atlas (TCGA) project (29) was exploited. There were 13 normal samples and 184 tumor samples in this dataset. Normalized miRNA expressions of miR-548c-3p were compared between normal and tumor samples. Mann-Whitney U test was applied to test the significance.

Survival analysis. A Kaplan-Meier curve was used to examine the clinical relevance of miR-548c-3p levels in the patients' outcomes (30). Patients were separated into two groups according to the median expression of hsa-miR-548c-3p using TCGA clinical and expression dataset. Differences between groups were analyzed using log-rank test (31) and two-tailed P-values <0.05 were considered statistically significant. Statistical analyses were performed using the survival package (version 2.39-5) in R (version 3.4.3).

Expression correlation of hsa-miR-548c-3p and its targeted genes. The miRNA and mRNA datasets of the esophageal carcinoma cohort from TCGA (29) were used for the correlation analysis. Common samples were isolated according to the sample barcodes. The Pearson correlation method was used to assess the expression association between hsa-miR-548c-3p and the targeted genes. Significance of association was determined by the R package cor.test (alternative='two.sided', method='pearson'). Then, P-values were corrected with Benjamini-Hochberg procedure for multiple testing.

Statistical analysis. All statistical analyses were generated using R (32). The Pearson correlation method was used to assess the expression association. Significances of associations were determined by the R package cor.test. Mann-Whitney U test was used for comparisons between two groups. Benjamini-Hochberg procedure was applied for multiple testing. Log-rank test was used for Kaplan-Meier survival curves. P<0.05 was considered to indicate a statistically significant difference.

Results

Identification of DE circRNAs in HCa. To identify DE circRNAs in HCa, circRNA sequencing (Seq) was performed using three matched normal and HCa tissue samples, and an average of 90 million reads was achieved for each sample. A total of 4,634 distinct circRNAs with at least two unique back-spliced reads across six samples using CIRI pipeline (13) were identified and the expressions of circRNAs were normalized and represented by reads per million mapped reads (RPM) values. Genetic distances across 6 samples were evaluated using PCA (Fig. 1A), and the normalized expression level (RPM) of circRNAs across the six samples is illustrated in Fig. 1B. Following statistical analysis, 71 and 102 circRNAs were determined to be significantly upregulated and downregulated, respectively

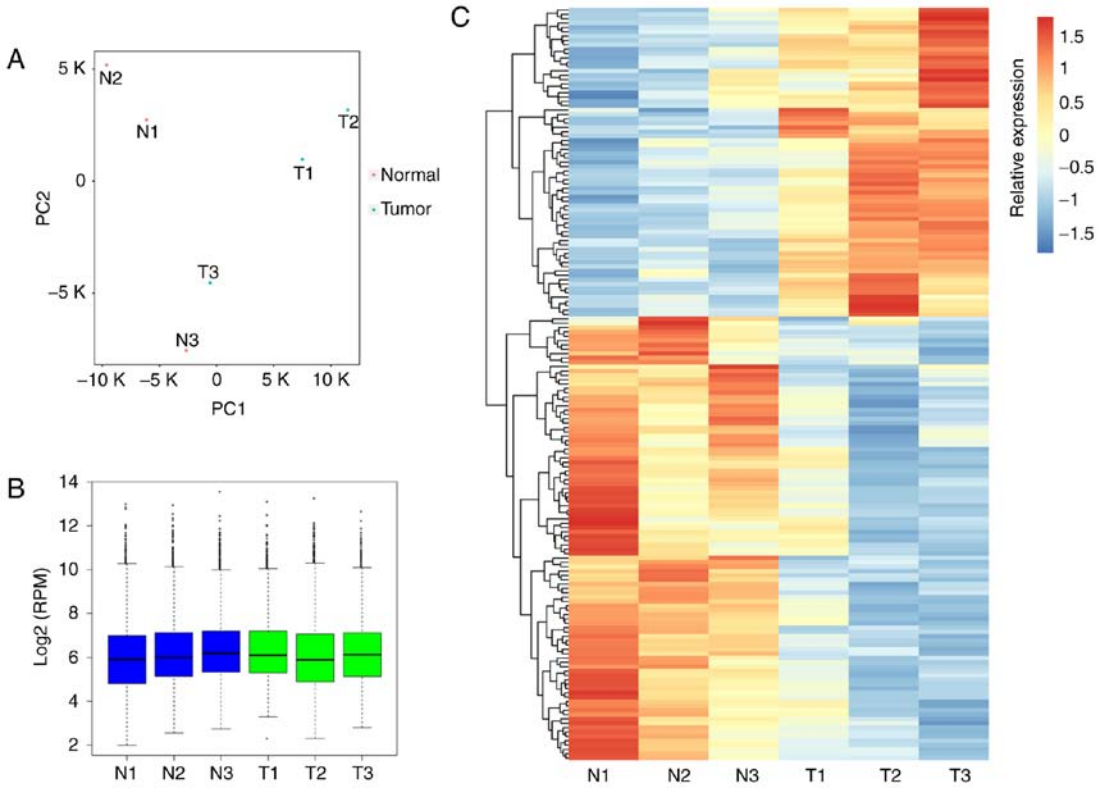

Figure 1. Identification of differentially expressed circRNAs in hypopharyngeal cancer. (A) PC analysis of three tumor samples and three normal samples using circRNA profiles. (B) Boxplot showing the log2 transformed back-spliced junction counts across adjacent normal and cancerous samples. (C) Heatmap of relative expression of differentially expressed circRNAs in adjacent normal and cancerous samples. circRNAs, circular RNAs; PC, principal component; N, normal; T, tumor.

(Table II). The DE circRNAs between tumor and adjacent normal samples were presented in a heatmap (Fig. 1C). To confirm the circRNA-Seq results, RT-qPCR was performed to assess the expression of 19 of the above DE circRNAs in both normal and tumor samples. The results confirmed that 12 of them were consistently upregulated or downregulated with the circRNA-Seq results (Fig. 2).

Next, the distribution of circRNAs in different DNA elements and chromosomes was examined. The bar diagram of Fig. 3A demonstrates the % of back-spliced junction reads on intron, intergenic, and exon areas. The majority of circRNAs belonged to exonic, followed by intronic and intergenic elements (Fig. 3B). These dysregulated circRNAs are widely distributed in all chromosomes, including sex chromosomes X (Fig. 3C).

Functional enrichment analysis of genes producing DE circRNAs. To reveal the dysregulated pathways underlying HCa, first KEGG pathway enrichment analyses were performed for genes that matched DE circRNAs. The results demonstrated that genes containing downregulated circRNAs were enriched in endocytosis, ubiquitin-mediated proteolysis, and Janus kinase (JAK)/signal transducer and activator of transcription (STAT) signaling pathways (Fig. 4A), whereas there were no KEGG pathways enriched with genes producing upregulated circRNAs.

Next, GO term enrichment analyies was performed for genes that produced aberrantly expressed circRNAs. Biological processes, such as the establishment of spindle orientation, response to fungicide, positive regulation of transcription, cell division were significantly enriched (Fig. 4B), whereas genes producing downregulated circRNAs were related to autophagy, mitochondrion organization actin cytoskeleton organization, membrane fission, and cell-cell adhesion pathways (Fig. 4C). These results suggested that multiple pathways may contribute to HCa pathogenesis and progression.

CircRNAs regulate the ErbB and Hippo pathways through a miRNA-CeRNA network. The role of circRNAs as a miRNA sponge is the main mechanism of circRNA function in tumor cells (11,33). Therefore, we further investigated the roles of circRNAs in HCa progression through establishing a ceRNA network. Firstly, the top 20 upregulated and top 20 downregulated circRNAs were isolated and were converted to circRNA ID using circBase database (34). Secondly, miRNAs targeting DE-circRNAs were isolated with the web server CircInteractome (23). Specifically, CircInteractome downloaded the mature sequences of all of the reported circRNAs from the UCSC browser, then to characterize miRNA-circRNA interactions, CircInteractome incorporated the ability to search using the TargetScan algorithm, which predicts miRNAs that target circRNA by surveying for 7-mer or 8-mer complementarity to the seed region as well as the 3'end of each miRNA (23). A total of 191 and 182 miRNAs were putatively identified as the targets of upregulated and downregulated circRNAs, respectively. Networks consisted of circRNAs and miRNAs were displayed using Cytoscape software (27). The results demonstrated extensive interactions

Table II. Differentially expressed circRNAs.

circRNA ID (CIRI)	circRNA ID (circBase)	Adjusted P-value	FC	Gene
chr16:21973780-21987564	hsa_circ_0005690	0.022002929	9.346453412	UQCRC2
chr2:242343242-242357524	hsa_circ_0004924	0.042106003	4.237176918	FARP2
chr7:72873865-72884813	hsa_circ_0004670	0.003579475	4.136199328	BAZ1B
chr5:133871547-133887899	hsa_circ_0005608	0.036132329	3.805820016	PHF15
chr22:41979962-41980607	hsa_circ_0005703	0.030406606	3.76275756	PMM1
chr3:48019354-48040369	hsa_circ_0005255	0.039183919	3.736266721	MAP4
chr12:27521194-27523163	hsa_circ_0009009	0.01165016	3.553331882	ARNTL2
chr9:117399269-117401006	hsa_circ_0002318	0.041159198	3.381349856	C9orf91
chr1:165859440-165860559	hsa_circ_0006758	0.041758958	3.367866028	UCK2
chr16:50321822-50322261	hsa_circ_0000699	0.043912028	3.314878392	ADCY7
chr16:89484691-89497734	hsa_circ_0000727	0.035411987	3.287797218	ANKRD11
chr8:98817580-98837381	hsa_circ_0003214	0.018483558	3.272900498	LAPTM4B
chr19:48229068-48229481	hsa_circ_0003146	0.006019062	3.268823068	EHD2
chr1:118003110-118045592	hsa_circ_0002059	0.010572316	3.169435071	MAN1A2
chr14:92264128-92268765	hsa_circ_0032969	0.040149042	3.130356466	TC2N
chr2:210968827-211019335	hsa_circ_0002617	0.020968937	3.121028088	C2orf67
chr15:94899365-94945248	hsa_circ_0000660	0.032292149	3.092238966	MCTP2
chr2:43655238-43657441	hsa_circ_0054309	0.002782953	3.091209609	THADA
chr2:110321942-110323436	hsa_circ_0009020	0.03917314	3.05906561	SEPT10
chr19:2137009-2138713	hsa_circ_0048344	0.040805597	3.048246172	AP3D1
chr16:4311779-4312702	hsa_circ_0002439	0.046240525	2.987845154	TFAP4
chr11:128993340-128997200	hsa_circ_0005027	0.001764073	2.945490868	ARHGAP32
chr8:62460629-62479877	hsa_circ_0084604	0.018794062	2.926235997	ASPH
chr3:155628480-155643155	hsa_circ_0008184	0.037854875	2.918397576	GMPS
chr16:47531309-47581459	hsa_circ_0004791	0.048387875	2.9019822	PHKB
chr20:35457456-35467844	hsa_circ_0060219	0.015622827	2.89815993	KIAA0889
chr3:195101737-195112876	hsa_circ_0007331	0.048715375	2.872843159	ACAP2
chr22:29517344-29521404	hsa_circ_0004547	0.044771757	2.802768657	KREMEN1
chr2:122260742-122287901	hsa_circ_0002374	0.037227807	2.731455995	CLASP1
chr3:128514202-128526514	hsa_circ_0006346	0.046003237	2.690296373	RAB7A
chr4:83793096-83796975	hsa_circ_0003549	0.044620973	2.679827252	SEC31A
chr12:1399017-1481143	hsa_circ_0024997	0.011882022	2.668639886	ERC1
chr13:96409897-96416207	#N/A	0.005392448	2.660521497	#N/A
chr16:30715384-30715636	hsa_circ_0039076	0.030665031	2.628113834	SRCAP
chr7:2400344-2404164	hsa_circ_0004869	0.033796697	2.611610945	EIF3B
chr2:55209650-55214834	hsa_circ_0001006	0.045899911	2.579018715	RTN4
chr12:42768664-42792796	hsa_circ_0003961	0.010866489	2.568055885	PPHLN1
chr7:2404006-2406083	hsa_circ_0001671	0.022907729	2.551488457	EIF3B
chr4:87685745-87689129	hsa_circ_0007948	0.022945704	2.547028768	PTPN13
chr1:176085759-176105683	hsa_circ_0015373	0.029930944	2.536801963	RFWD2
chr22:36737414-36745300	hsa_circ_0004470	5.2192E-05	2.529021894	MYH9
chr2:32396355-32409407	hsa_circ_0053423	0.031086982	2.514457353	SLC30A6
chr7:138951078-138957186	hsa_circ_0005594	0.027733961	2.504492053	UBN2
chr9:95030455-95032265	hsa_circ_0008367	0.016513149	2.486273648	IARS
chr7:65705311-65751696	hsa_circ_0006041	0.005514578	2.410252357	TPST1
chr4:75040222-75067087	hsa_circ_0069981	0.032657959	2.370951734	MTHFD2L
chr1:246021797-246093239	hsa_circ_0017289	0.010842885	2.366575966	SMYD3
chr22:29090019-29091861	hsa_circ_0004811	0.001831625	2.363098777	CHEK2
chr16:3900297-3901010	hsa_circ_0007637	0.009154577	2.351311388	CREBBP
chr2:168920009-168931741	hsa_circ_0003279	0.000393597	2.342009076	STK39
chr10:101728871-101731891	hsa_circ_0008393	0.049564434	2.328443205	DNMBP
chr9:140646782-140652463	hsa_circ_0001904	0.031745459	2.316860866	EHMT1

Table II. Continued.

circRNA ID (CIRI)	circRNA ID (circBase)	Adjusted P-value	FC	Gene
chr22:46125304-46136418	hsa_circ_0001247	0.013526942	2.31185877	ATXN10
chr14:23419522-23421892	hsa_circ_0005663	0.04538212	2.257072167	HAUS4
chr12:122773035-122801402	#N/A	0.015647694	2.25006903	#N/A
chr4:3188323-3190820	#N/A	0.025850456	2.249708035	#N/A
chr3:172363412-172365904	hsa_circ_0007042	0.026989758	2.238835674	NCEH1
chr2:10799297-10808849	hsa_circ_0008511	0.042758286	2.221921485	NOL10
chr10:70696691-70703013	hsa_circ_0007097	0.040819924	2.219586601	DDX50
chrX:14868626-14877456	hsa_circ_0006971	0.009211245	2.215797457	FANCB
chr1:23356961-23385660	hsa_circ_0007822	0.027240129	2.206406433	KDM1A
chr20:13539654-13561628	hsa_circ_0002001	0.017808498	2.188222168	TASP1
chr7:139741443-139757834	hsa_circ_0004684	0.026813206	2.168759032	PARP12
chr7:72883846-72884813	hsa_circ_0003866	0.012904268	2.108744306	BAZ1B
chr1:247319707-247323115	#N/A	0.039522611	2.102327859	#N/A
chr18:21644103-21663045	hsa_circ_0047270	0.020649137	2.07972359	TTC39C
chr1:31532050-31532424	hsa_circ_0000045	0.009259898	2.078191163	PUM1
chr2:63660878-63667005	hsa_circ_0003497	0.033526319	2.072706608	WDPCP
chr10:128859931-128908618	hsa_circ_0020462	0.014021298	2.068064026	DOCK1
chr1:44773981-44804994	hsa_circ_0007693	0.022406409	2.066977275	ERI3
chr7:99621041-99621930	hsa_circ_0001727	0.043987221	2.025308683	ZKSCAN1
chr16:11873021-11876244	hsa_circ_0005420	0.045974717	0.499738449	ZC3H7A
chr20:13539654-13561628	hsa_circ_0002001	0.03937226	0.497281358	TASP1
chr3:43341245-43345284	hsa_circ_0004089	0.007985302	0.491228173	SNRK
chrX:77084527-77086392	#N/A	0.020792399	0.489952895	#N/A
chr2:11905658-11907984	hsa_circ_0002229	0.013904514	0.48799699	LPIN1
chr17:60111147-60112969	hsa_circ_0004273	0.010727519	0.487251947	MED13
chr2:168920009-168986268	hsa_circ_0005882	0.018253559	0.481253188	STK39
chr16:53532302-53534241	hsa_circ_0004072	0.021867418	0.480875236	AKTIP
chr9:95030455-95032265	hsa_circ_0008367	0.024608207	0.480576493	IARS
chr9:14146687-14179779	hsa_circ_0086376	0.025017135	0.480402794	NFIB
chr12:122773035-122801402	#N/A	0.027697748	0.475833919	#N/A
chr20:35457456-35467844	hsa_circ_0060219	0.01965515	0.472752875	KIAA0889
chr15:80412669-80415142	hsa_circ_0000643	0.019656594	0.47081423	ZFAND6
chr4:144449020-144451679	#N/A	0.002041818	0.470785346	#N/A
chr15:62299506-62306191	hsa_circ_0000607	0.01862274	0.47022119	VPS13C
chr21:40578033-40584633	#N/A	0.038815333	0.466807062	#N/A
chr10:128859931-128908618	hsa_circ_0020462	0.048526313	0.46671725	DOCK1
chr1:32381495-32385259	hsa_circ_0007364	0.012904962	0.464916349	PTP4A2
chr2:148811959-148990964	#N/A	0.018584205	0.463574046	#N/A
chr8:37734626-37735069	hsa_circ_0001789	0.019846769	0.462223466	RAB11FIP1
chr13:28748408-28752072	hsa_circ_0004372	0.023765765	0.461563778	PAN3
chr18:9931806-9937063	hsa_circ_0006990	0.039623112	0.461171429	VAPA
chr17:34910660-34923615	hsa_circ_0003930	0.021748331	0.458221861	GGNBP2
chr22:46125304-46136418	hsa_circ_0001247	0.008045429	0.453521935	ATXN10
chr2:206992520-206994966	hsa_circ_0002431	0.036437006	0.452588631	NDUFS1
chr2:62100136-62103369	hsa_circ_0001018	0.029799501	0.451702188	CCT4
chr11:119144577-119145663	hsa_circ_0000362	0.025621724	0.450849769	CBL
chr4:39734978-39747430	#N/A	0.03460933	0.450272258	#N/A
chr22:29682911-29683123	hsa_circ_0008044	0.010096395	0.44308523	EWSR1
chr14:21971315-21972024	hsa_circ_0000523	0.047512563	0.44023344	METTL3
chr14:50615002-50616948	#N/A	0.013896814	0.437352627	#N/A
chr8:101232506-101243516	#N/A	0.028204026	0.430720792	#N/A
chr7:72883846-72884813	hsa_circ_0003866	0.004390368	0.424421462	BAZ1B

Table II. Continued.

circRNA ID (CIRI)	circRNA ID (circBase)	Adjusted P-value	FC	Gene
chr18:46858233-46906128	hsa_circ_0002501	0.03573514	0.420126159	DYM
chr1:246784730-246797889	hsa_circ_0017311	0.028462249	0.41970008	CNST
chr12:1399017-1481143	hsa_circ_0024997	0.040174171	0.417295868	ERC1
chr12:27521194-27523163	hsa_circ_0009009	0.024711114	0.414722924	ARNTL2
chr1:52959282-52975384	hsa_circ_0003632	0.045708435	0.414593811	ZCCHC11
chr5:50055476-50059076	hsa_circ_0006787	0.018488474	0.412395338	PARP8
chr3:179096128-179104417	hsa_circ_0002219	0.029224282	0.403006229	MFN1
chr10:88203031-88206206	#N/A	0.022884862	0.399217754	#N/A
chr17:26490568-26499644	hsa_circ_0003638	0.013335258	0.397922038	NLK
chr16:8952206-8953192	hsa_circ_0000669	0.000715169	0.397901388	CARHSP1
chr2:186946056-186964557	#N/A	0.017444656	0.397798992	#N/A
chr11:85685750-85695016	hsa_circ_0006629	0.01991069	0.396956177	PICALM
chr7:91980263-91991587	#N/A	0.035701238	0.389282593	#N/A
chr14:35519989-35522657	hsa_circ_0006424	0.04322634	0.387507944	FAM177A1
chr12:42768664-42792796	hsa_circ_0003961	0.014465456	0.386034041	PPHLN1
chr1:246021797-246093239	hsa_circ_0017289	0.011181456	0.38452595	SMYD3
chr10:27431315-27434519	hsa_circ_0005633	0.009131314	0.384171219	YME1L1
chr12:129299319-129299615	hsa_circ_0000462	0.006941025	0.380095649	SLC15A4
chr1:118003110-118045592	hsa_circ_0002059	0.002220417	0.379882753	MAN1A2
chr6:55966269-56006781	#N/A	0.022261578	0.375691727	#N/A
chr8:17123415-17126465	hsa_circ_0008592	0.040012263	0.373149729	VPS37A
chr10:99915849-99923154	hsa_circ_0004419	0.032103617	0.372519687	C10orf28
chr20:17933230-17934761	hsa_circ_0006704	0.020560715	0.371748201	SNX5
chr1:31532050-31532424	hsa_circ_0000045	0.040901772	0.368955101	PUM1
chrX:14868626-14877456	hsa_circ_0006971	0.032386045	0.36887067	FANCB
chr16:3900297-3901010	hsa_circ_0007637	0.020340132	0.36603697	CREBBP
chr4:103644027-103647840	hsa_circ_0006007	0.02570568	0.359726565	MANBA
chr1:62907158-62907970	#N/A	0.047427014	0.35583852	#N/A
chr18:18619432-18624147	hsa_circ_0006733	0.037595523	0.353388689	ROCK1
chr14:52977957-53011089	hsa_circ_0031939	0.01966747	0.351937505	TXNDC16
chr21:37711076-37717005	hsa_circ_0001189	0.010082196	0.351308477	MORC3
chr1:94685813-94697199	hsa_circ_0003310	0.0259611	0.351119971	ARHGAP29
chr3:47103652-47108608	hsa_circ_0065159	0.020521933	0.350064342	SETD2
chr8:71126137-71128999	#N/A	0.048201309	0.344144613	#N/A
chr16:71779046-71779517	hsa_circ_0002505	0.046185136	0.343484211	AP1G1
chr5:31421378-31424578	hsa_circ_0005524	0.044966353	0.34303411	DROSHA
chr11:1307231-1317024	hsa_circ_0008301	0.018942131	0.342187543	TOLLIP
chr6:108242132-108243113	#N/A	0.012934139	0.340934595	#N/A
chr19:48229068-48229481	hsa_circ_0003146	0.020562164	0.340720207	EHD2
chr3:37170553-37190529	hsa_circ_0003264	0.013154932	0.336803278	LRRFIP2
chr7:65705311-65751696	hsa_circ_0006041	0.039282961	0.334902033	TPST1
chr13:96409897-96416207	#N/A	0.0177537	0.332540513	#N/A
chr8:68200189-68214701	#N/A	0.011526157	0.328702879	#N/A
chr7:27668989-27689252	hsa_circ_0006773	0.003935998	0.328463848	HIBADH
chr10:32308785-32310215	hsa_circ_0006408	0.043640924	0.325878207	KIF5B
chr7:77407654-77408131	#N/A	0.023396605	0.323146621	#N/A
chr3:56600621-56601081	hsa_circ_0001312	0.029755856	0.321652942	CCDC66
chr2:234271722-234299129	#N/A	0.02313964	0.321131598	#N/A
chr7:73100965-73101425	hsa_circ_0005588	0.042073587	0.318524548	WBSCR22
chr7:72873865-72884813	hsa_circ_0004670	0.043342921	0.316315928	BAZ1B
chr2:242282406-242283312	hsa_circ_0059060	0.007810999	0.315723287	SEPT2
chr3:47139444-47144913	hsa_circ_0001289	0.039274732	0.313502465	SETD2

Table II. Continued.

circRNA ID (CIRI)	circRNA ID (circBase)	Adjusted P-value	FC	Gene
chr2:43655238-43657441	hsa_circ_0054309	0.038540875	0.309703944	THADA
chr21:46275124-46281186	hsa_circ_0001200	0.0474882	0.302025085	PTTG1IP
chr5:179976930-179980471	hsa_circ_0008836	0.028790905	0.292442462	CNOT6
chr1:87185189-87190088	hsa_circ_0013084	0.01567065	0.280991627	SH3GLB1
chr19:53577392-53578436	hsa_circ_0007480	0.031784533	0.275005495	ZNF160
chr16:53289511-53297009	#N/A	0.003705027	0.260024152	#N/A
chr22:29090019-29091861	hsa_circ_0004811	0.008438851	0.252361922	CHEK2
chrX:117718697-117724265	hsa_circ_0091382	0.032765014	0.247214419	DOCK11
chr11:128993340-128997200	hsa_circ_0005027	0.041341275	0.246885645	ARHGAP32
chr15:34542498-34543258	hsa_circ_0034346	0.039707643	0.246690583	SLC12A6
chr10:70152894-70154208	hsa_circ_0000239	0.008512372	0.236281903	RUFY2
chr1:236966727-236979843	#N/A	0.036146024	0.222019071	#N/A
chr19:33604672-33605325	hsa_circ_0008287	0.042162087	0.207707068	GPATCH1
chr2:168920009-168931741	hsa_circ_0003279	0.001767352	0.196582978	STK39
chr1:179087721-179091002	#N/A	0.019369988	0.169662407	#N/A
chr18:9524591-9525849	hsa_circ_0005158	0.043392731	0.166193525	RALBP1
chr22:36737414-36745300	hsa_circ_0004470	0.042494836	0.147382721	MYH9

The criteria for the differential expression were: Adjusted P<0.05 and FC>2 or FC<0.5. The top 20 upregulated and downregulated genes are presented in bold. circRNA, circular RNA; FC, fold change.

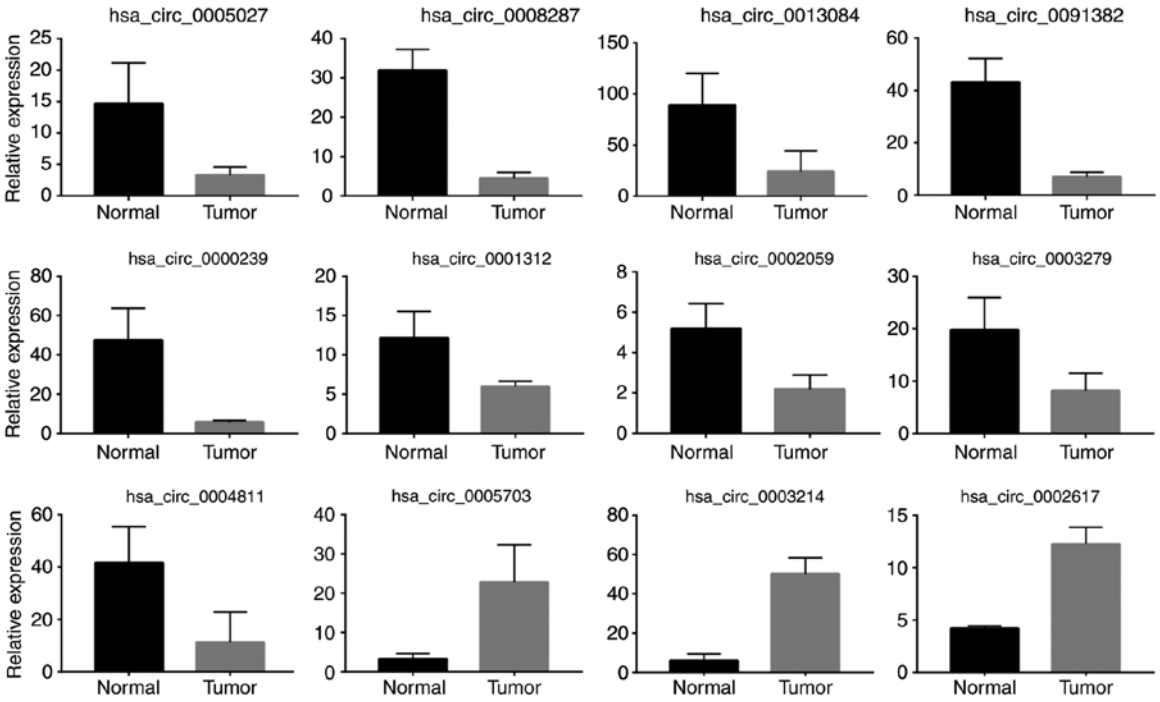

Figure 2. Reverse transcription-quantitative polymerase chain reaction analysis. Twelve of 19 circRNAs were demonstrated to be consistently regulated with the circRNA-sequencing results. circRNAs, circular RNAs.

between miRNAs and upregulated (Fig. 5A), and downregulated circRNAs (Fig. 5B). Then, KEGG pathway enrichment analysis was performed for the miRNAs targeted by the top 40 DE circRNAs, in order to explore the altered biological processes using mirPath 3.0 (26). Genes targeted by miRNAs were significantly enriched in multiple signaling pathways, including the ErbB, the Hippo, the Ras, the transforming growth factor (TGF)-β, the phosphoinositide 3-kinase/AKT serine/threonine kinase and the Wnt signaling pathways (Fig. 5C).

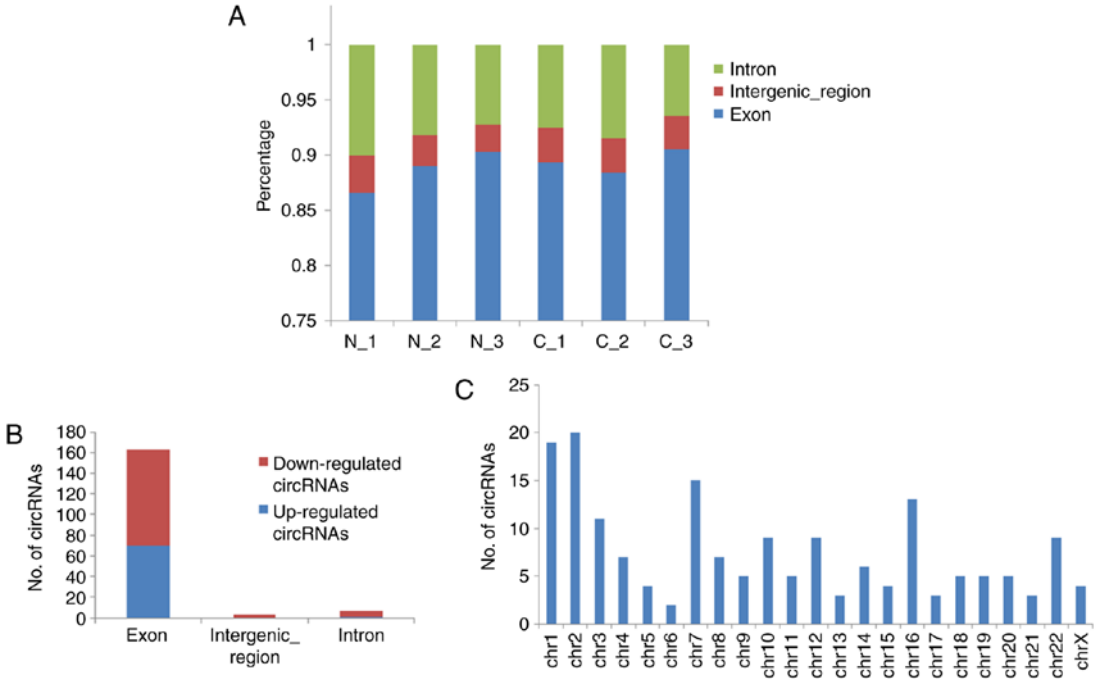

Figure 3. Distribution of circRNAs in different DNA elements and chromosomes. (A) Bar diagram showing the % of back-spliced junction reads of circRNAs on genome elements. (B) Distribution of upregulated and downregulated circRNAs according to genome elements. (C) Distribution of numbers of differentially expressed circRNAs across the 23 chromosomes. circRNAs, circular RNAs; chr, chromosome.

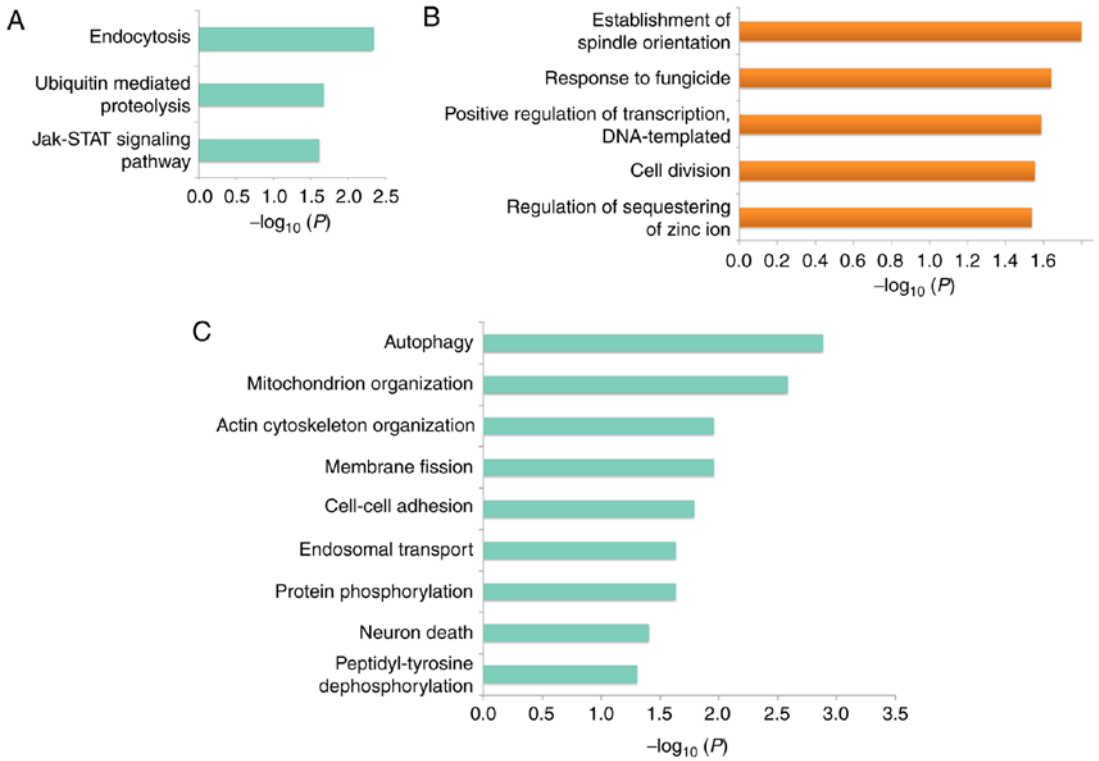

Figure 4. GO and KEGG pathway enrichment analyses. (A) KEGG pathway enrichment analysis of the genes that produced downregulated circRNAs. (B) GO enrichment analyses of genes that produced upregulated and (C) downregulated circRNAs. The blue bars denote the biological processes of genes producing downregulated circRNAs, while the orange bars denote the biological processes of genes producing upregulated circRNAs. GO, gene ontology; KEGG, Kyoto Encyclopedia of Genes and Genomes; circRNAs, circular RNAs.

To get further insight into the function of circRNAs in the ErbB and Hippo signaling pathways, miRNA-ceRNA networks were constructed corresponding to the two pathways using Cytoscape. For the miRNA-ceRNA network regulating the ErbB pathway, there were 33 circRNAs, 43 miRNAs and 74 ErbB pathway genes (Fig. 6A). In the ErbB miRNA-ceRNA

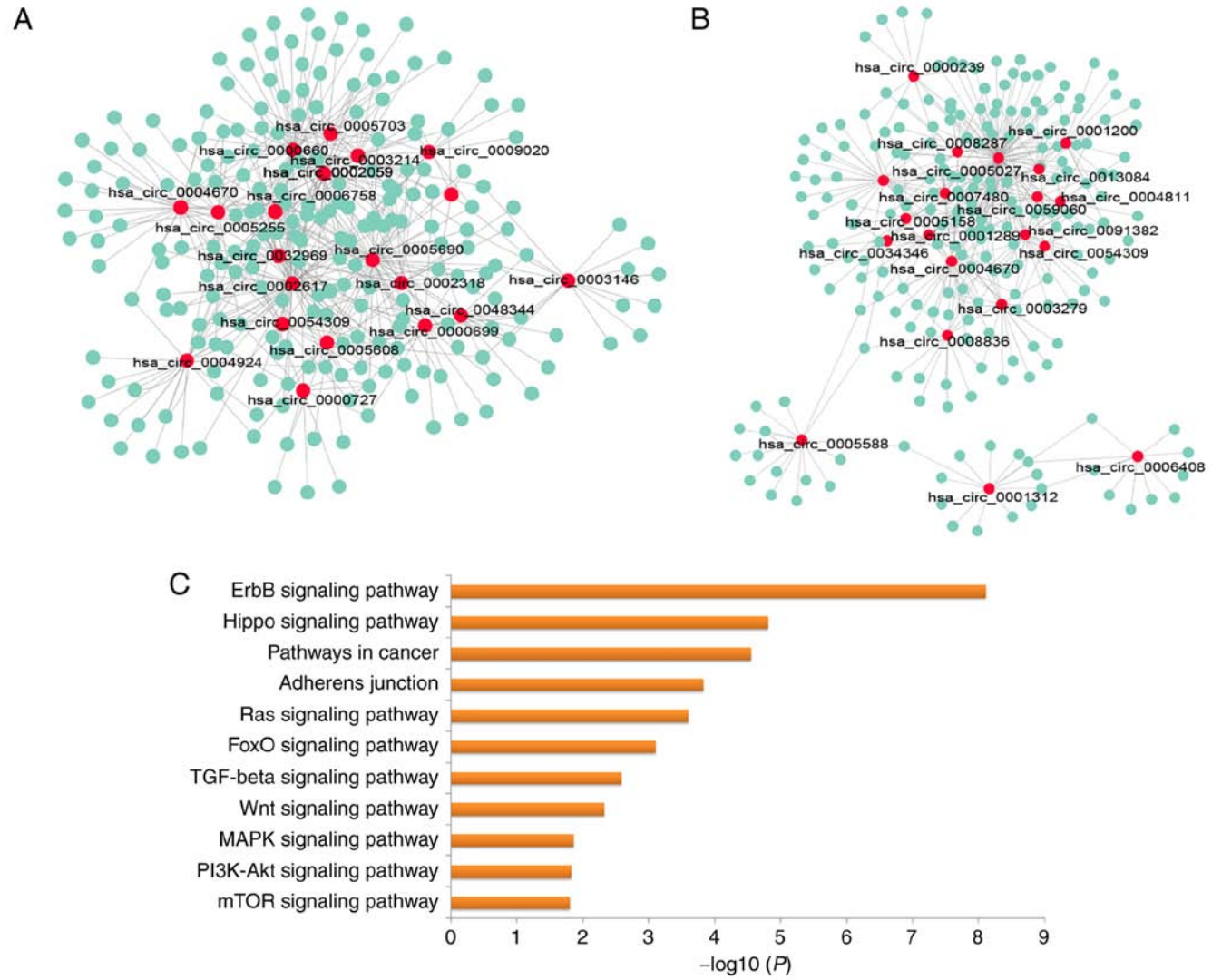

Figure 5. miRNA-ceRNA network. (A) Upregulated circRNAs/miRNAs ceRNA network. (B) Downregulated circRNAs/miRNAs ceRNA network. The red nodes represent circRNAs and the green nodes represent miRNAs. (C) KEGG pathway enrichment analysis of miRNAs. miRNA, microRNA; ceRNA, competing endogenous RNA; circRNAs, circular RNAs; KEGG, Kyoto Encyclopedia of Genes and Genomes.

network, we isolated a subnetwork consisting of circRNAs (hsa_circ_0008287 and hsa_circ_0005027), miRNAs (hsa-miR-548c-3p) and 38 ErbB pathway genes which had the most interaction between miRNAs and targeted genes (Fig. 6B). Hsa_circ_0008287 and hsa_circ_0005027 were significantly downregulated in tumor samples compared with normal (Figs. 2 and 6C). In a similar manner, the miRNA-ceRNA network regulating the Hippo pathway was constructed, consisting of 33 circRNAs, 43 miRNAs and 110 Hippo pathway genes (Fig. 7A). In the Hippo miRNA-ceRNA network, we also isolated a subnetwork consisting of circRNAs (hsa_circ_0008287 and hsa_circ_0005027), miRNAs (hsa-miR-548c-3p) and 61 Hippo pathway genes, which had the most interaction between miRNAs and targeted genes (Fig. 7B).

To further investigate the important role of this subnetwork in tumor progression, the miRNA and mRNA datasets of the esophageal carcinoma cohort from TCGA (29) were exploited. The esophageal carcinoma cohort contains 13 normal samples and 184 tumor samples. In this cohort, the miRNA hsa-miR-548c-3p expression between normal and tumor samples was detected, and its clinical relevance to patient survival was analyzed. The results suggested that hsa-miR-548c-3p was highly expressed in tumor samples compared with normal samples (Fig. 8A and B), and its high expression was significantly associated with lower survival in patients with esophageal carcinoma (Fig. 8C). These findings suggested that hsa-miR-548c-3p is an oncogenic miRNA, which is consistent with the hypothesis that in tumor samples circRNAs were downregulated resulting in more oncogenic hsa-miR-548c-3p being released, and highly expressed hsa-miR-548c-3p may promote HCa progression through downstream target genes. To confirm the negative regulation of hsa-miR-548c-3p on the ErbB and Hippo pathway genes, the expression correlation of hsa-miR-548c-3p and its targeted genes were also analyzed. Many of the targeted genes were negatively correlated with hsa-miR-548c-3p levels, which supported a negative regulatory role of hsa-miR-548c-3p on the ErbB and Hippo pathways (Table III). The present results demonstrated that circRNAs regulate HCa progression through multiple pathways and identifying a miRNA-ceRNA network that regulated the ErbB and Hippo signaling pathways.

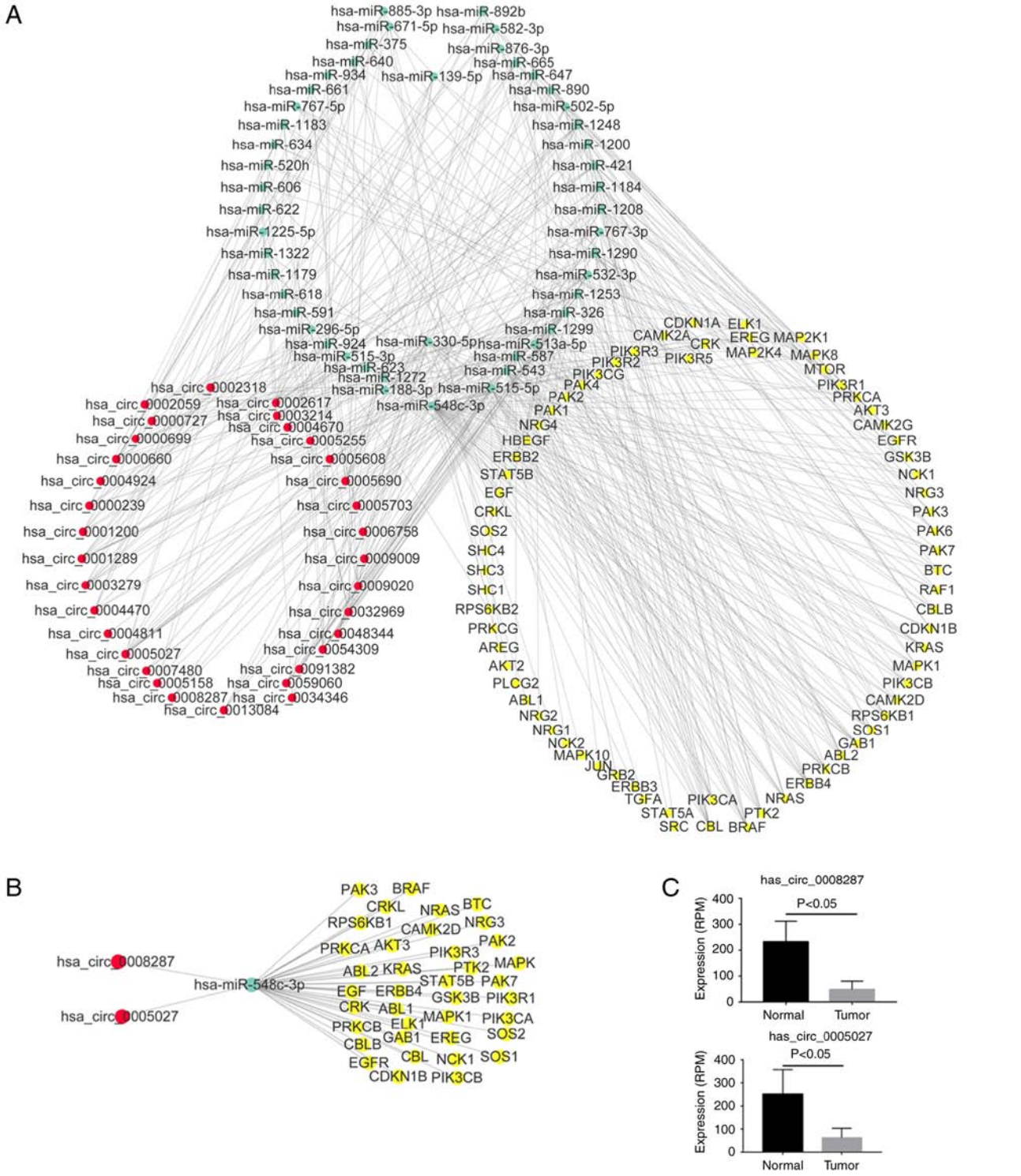

Figure 6. Involvement of circRNAs in the ErbB signaling pathway. (A) miRNA-ceRNA network of the ErbB signaling pathway. (B) Subnetwork consisting of circRNAs (hsa_circ_0008287 and hsa_circ_0005027)/miRNAs (hsa-miR-548c-3p) and ErbB pathway genes. (C) hsa_circ_0008287 and hsa_circ_0005027 were downregulated in tumor samples (circRNA-Sequencing results). circRNAs, circular RNAs; miRNA, microRNA; ceRNA, competing endogenous RNA.

Discussion

HCa is clinically difficult to diagnose and has a poor prognosis, therefore, identifying early stage molecular biomarkers has become urgent. CircRNAs, which are stable and easier to extract and detect, are considered ideal candidates for early-stage biomarkers. This is the first report on the expression profile of circRNAs in HCa. In the present study, a number of aberrantly expressed circRNAs in HCa samples were identified. Pathway enrichment results revealed that circRNAs may regulate HCa progression through multiple signaling pathways, especially the ErbB and Hippo signaling pathways. These results provided several potential biomarkers and therapeutic targets for HCa.

The ceRNA hypothesis was described as a way that RNAs communicate with each other, via competing for

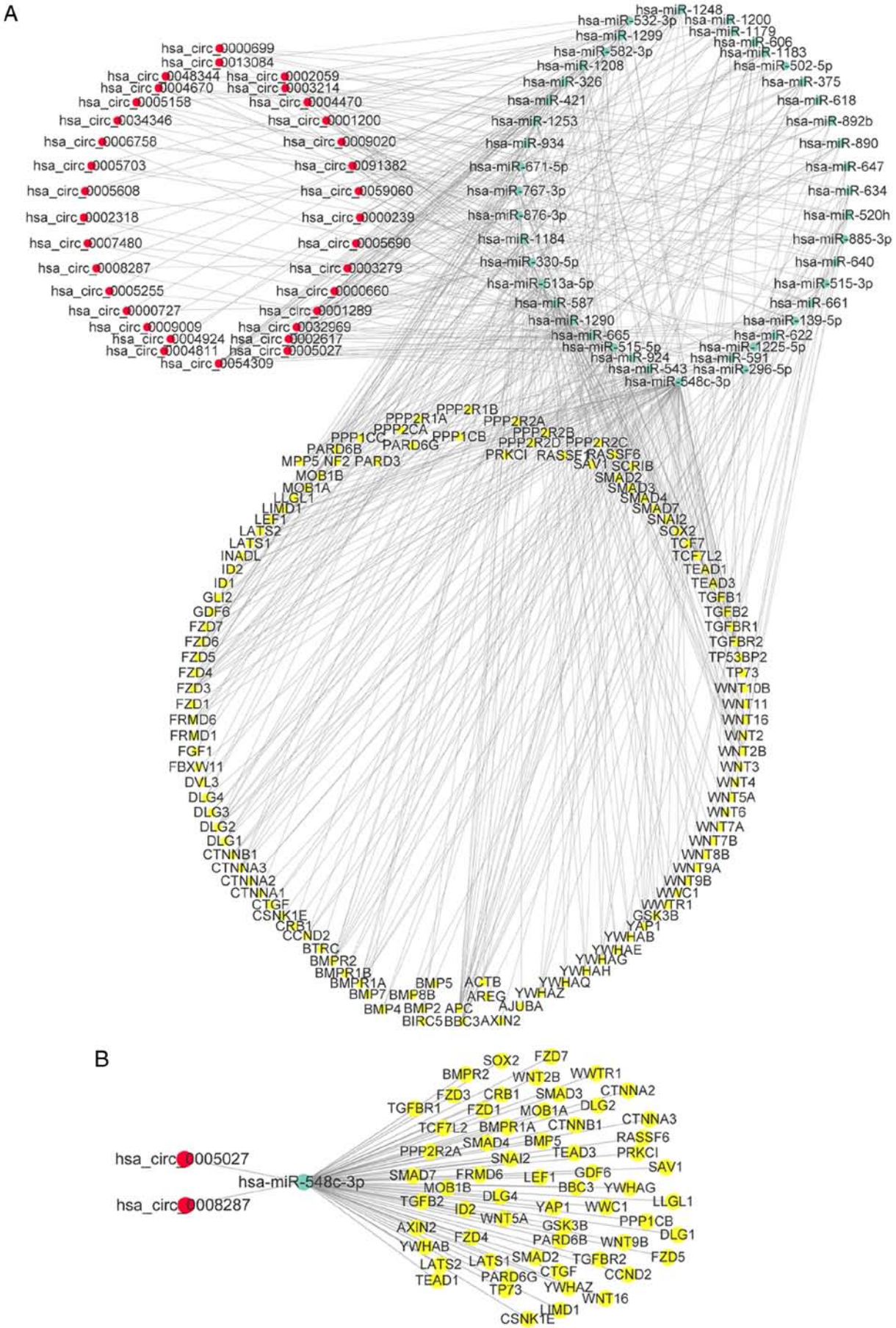

Figure 7. Involvement of circRNAs in the Hippo signaling pathway. (A) miRNA-ceRNA network of Hippo signaling pathway. (B) Subnetwork consisting of circRNAs (hsa_circ_0008287 and hsa_circ_0005027)/miRNAs (hsa-miR-548c-3p) and Hippo pathway genes. circRNAs, circular RNAs; miRNA, microRNA; ceRNA, competing endogenous RNA.

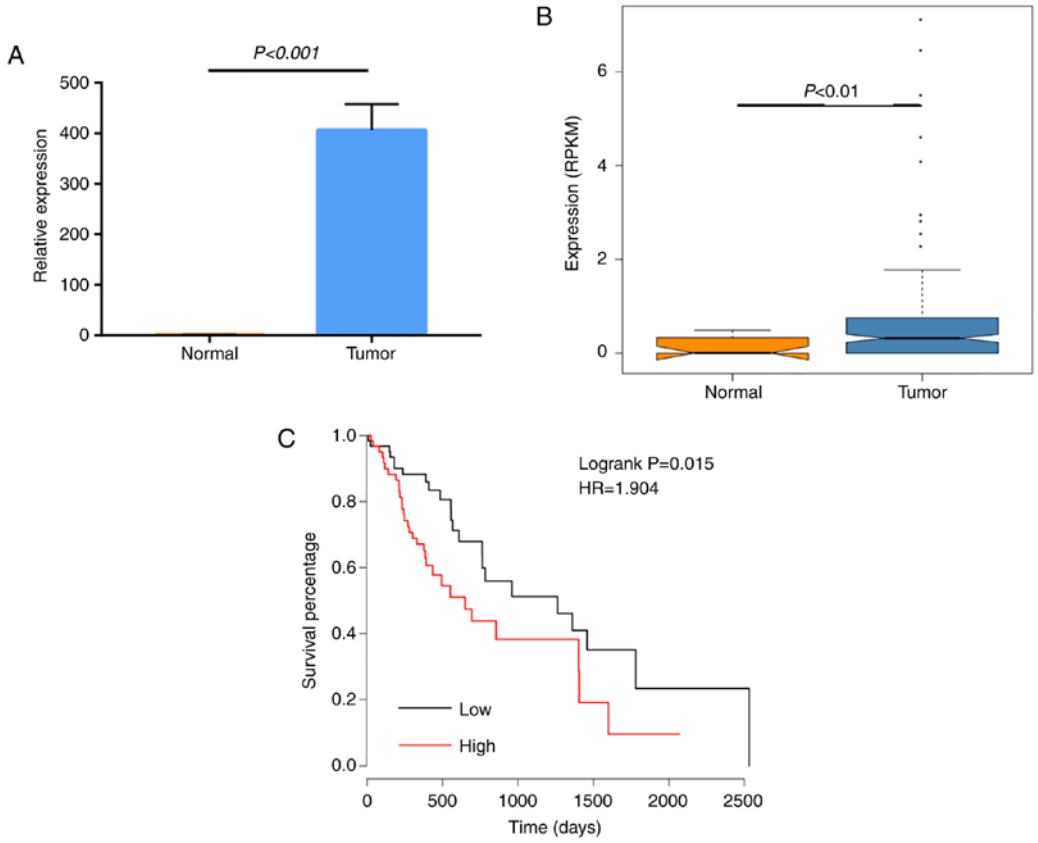

Figure 8. hsa-miR-548c-3p expression in esophageal carcinoma and its association to patient survival. (A) Expression of hsa-miR-548c-3p between normal and tumor samples from patients with hypopharyngeal cancer, by reverse transcription-quantitative polymerase chain reaction analysis. Three technical replicates were used. (B) Expression of hsa-miR-548c-3p between normal and tumor samples of esophageal carcinoma, by in-silico analysis. The miRNA dataset of the esophageal carcinoma cohort from The Cancer Genome Atlas project was used for the analysis. (C) Kaplan-Meier plot of overall survival in patients with high or low expression of hsa-miR-548c-3p. miRNA, microRNA.

binding to miRNAs and regulating the expression of each other to construct a complex post-transcriptional regulatory network (35,36). mRNAs and long non-coding (lnc) RNAs may all serve as ceRNAs (37). It has been demonstrated that circRNAs can also function as miRNA sponges (6,11). The present study demonstrated that aberrantly expressed circRNAs have extensive interactions with miRNAs, and those miRNAs exerted their effect on multiple cancer-related pathways. These data indicated that the circRNA-associated ceRNA network may have crucial roles in HCa progression.

The activation of ErbB oncogenes has been described in various types of human tumors, including hypopharynx carcinomas, and it has been correlated with a poor prognosis. For example, one study describing the molecular alterations in hypopharynx carcinomas demonstrated that ErbB1 was amplified in 29% of patients with hypopharyngeal squamous cell carcinomas (38). In addition, ErbB1 amplification is correlated with a hypopharyngeal primary site (39). Another study reported that v-erbB stained positively in 62.5% of hypopharyngeal squamous cell carcinomas samples but negatively in normal mucosa (40). The present ceRNA network analysis demonstrated that a circRNA (hsa_circ_0008287 and hsa_circ_0005027)/miRNA (hsa-miR-548c-3p) axis may have important roles in ErbB-mediated tumor progression (Fig. 6).

Another pathway that is likely to be associated with hypopharynx carcinomas is the Hippo signaling pathway. The Hippo pathway has generated considerable interest in recent years because of its involvement in several key hallmarks of cancer progression and metastasis (41). Regulation of Hippo signaling can be an attractive alternative strategy for cancer treatment (42-44). Previously, ACTL6A and p63 were demonstrated to cooperatively promote head and neck squamous cell carcinoma, through activation of the Hippo/Yes-associated protein 1 (YAP) pathway and YAP activation can predict poor patient survival (45). The present ceRNA network analysis demonstrated that a circRNA (hsa_circ_0008287 and hsa_circ_0005027)/miRNA (hsa-miR-548c-3p) axis may have important roles in Hippo-mediated tumor progression (Fig. 7).

Extensive evidence has suggested that miRNAs have important roles in breast cancer. The miR-548 family has been demonstrated to be involved in the pathogenesis of several cancers. For example, miR-548-3p was significantly downregulated in breast cancer and overexpression of miR-548-3p inhibited the proliferation and promoted the apoptosis of breast cancer cells (46). Overexpression of miR-548c-3p was also confirmed in prostate epithelial stem cells and in castration-resistant prostate cancer cells (45). Overexpression of miR-548c-3p in differentiated cells induced stem-like properties and radioresistance (45). Re-analyses of published studies further revealed that miR-548c-3p is significantly overexpressed

Table III. Expression correlation of hsa-miR-548c-3p and its targeted genes in The Cancer Genome Atlas esophageal carcinoma cohort.

miRNA	Gene	Correlation coefficient	FDR
hsa-miR-548c-3p	PIK3CA	-0.179442021	0.011633
hsa-miR-548c-3p	ABL1	-0.16430793	0.021044
hsa-miR-548c-3p	PIK3R1	-0.159510982	0.025159
hsa-miR-548c-3p	AKT3	-0.152832805	0.032027
hsa-miR-548c-3p	CTGF	-0.139434991	0.050682
hsa-miR-548c-3p	DLG2	-0.136001942	0.056703
hsa-miR-548c-3p	FRMD6	-0.128579884	0.07175
hsa-miR-548c-3p	GAB1	-0.119111167	0.095493
hsa-miR-548c-3p	GDF6	-0.114236586	0.109949
hsa-miR-548c-3p	BTC	-0.114017567	0.110637
hsa-miR-548c-3p	CCND2	-0.113880294	0.11107
hsa-miR-548c-3p	SOS2	-0.106454244	0.136518
hsa-miR-548c-3p	ABL2	-0.103988246	0.14589
hsa-miR-548c-3p	STAT5B	-0.103173372	0.149092
hsa-miR-548c-3p	ERBB4	-0.099703628	0.163324
hsa-miR-548c-3p	CBLB	-0.083838426	0.241477
hsa-miR-548c-3p	DLG4	-0.083217471	0.244993
hsa-miR-548c-3p	BMPR1A	-0.082135258	0.251205
hsa-miR-548c-3p	PAK7	-0.079722196	0.265448
hsa-miR-548c-3p	DLG1	-0.072417936	0.311876
hsa-miR-548c-3p	CAMK2D	-0.070087122	0.327746
hsa-miR-548c-3p	LEF1	-0.068131773	0.341454
hsa-miR-548c-3p	CTNNA3	-0.06669216	0.351776
hsa-miR-548c-3p	PAK2	-0.066482615	0.353295
hsa-miR-548c-3p	PTK2	-0.064644262	0.366794
hsa-miR-548c-3p	FZD1	-0.063827484	0.372892
hsa-miR-548c-3p	NRG3	-0.053532783	0.454989
hsa-miR-548c-3p	LATS2	-0.052315837	0.46532
hsa-miR-548c-3p	RPS6KB1	-0.049387268	0.490702
hsa-miR-548c-3p	NCK1	-0.047228889	0.509871
hsa-miR-548c-3p	PRKCB	-0.045059635	0.529521
hsa-miR-548c-3p	FZD4	-0.041762665	0.560101
hsa-miR-548c-3p	LLGL1	-0.037399843	0.601828
hsa-miR-548c-3p	BMPR2	-0.036025864	0.615251
hsa-miR-548c-3p	GSK3B	-0.022579459	0.752806
hsa-miR-548c-3p	GSK3B	-0.022579459	0.752806
hsa-miR-548c-3p	EGFR	-0.019225787	0.788581
hsa-miR-548c-3p	PRKCA	-0.017068489	0.811834
hsa-miR-548c-3p	LATS1	-0.014844376	0.835982
hsa-miR-548c-3p	FZD7	-0.012434723	0.862317
hsa-miR-548c-3p	PAK3	-0.012235276	0.864504
hsa-miR-548c-3p	BRAF	-0.011521175	0.872343
hsa-miR-548c-3p	SOS1	-0.007706896	0.914404
hsa-miR-548c-3p	CBL	-0.006374831	0.929156
hsa-miR-548c-3p	CRKL	-0.005591422	0.937844
hsa-miR-548c-3p	BMP5	-0.004257302	0.952654
hsa-miR-548c-3p	EGF	0.000395288	0.995601
hsa-miR-548c-3p	PIK3CB	0.002839251	0.968414
hsa-miR-548c-3p	MAPK8	0.021309033	0.766301
hsa-miR-548c-3p	CRK	0.031385585	0.661515
hsa-miR-548c-3p	LIMD1	0.031613315	0.659213
hsa-miR-548c-3p	CRB1	0.032804274	0.647223
hsa-miR-548c-3p	FZD3	0.040937544	0.567885
hsa-miR-548c-3p	PIK3R3	0.041780747	0.559931
hsa-miR-548c-3p	KRAS	0.056284445	0.43211
hsa-miR-548c-3p	CTNNB1	0.057967563	0.418448
hsa-miR-548c-3p	NRAS	0.065278707	0.362099
hsa-miR-548c-3p	CDKN1B	0.0732999	0.306004
hsa-miR-548c-3p	MAPK1	0.083215756	0.245003
hsa-miR-548c-3p	EREG	0.086515941	0.226721
hsa-miR-548c-3p	BBC3	0.102224529	0.152888
hsa-miR-548c-3p	ELK1	0.115802515	0.105129
hsa-miR-548c-3p	CSNK1E	0.137981222	0.053163
hsa-miR-548c-3p	AXIN2	0.158253961	0.026346
hsa-miR-548c-3p	FZD5	0.169685512	0.017135
hsa-miR-548c-3p	ID2	0.202596669	0.004302
hsa-miR-548c-3p	CTNNA2	0.246858375	0.00047

Table III. Continued.

miRNA, microRNA; FDR, false discovery rate.

in castration-resistant prostate cancer cells and is associated with poor recurrence-free survival, suggesting that miR-548c-3p is a functional biomarker for prostate cancer aggressiveness (47). The present results demonstrated that miR-548c-3p may have important roles in HCa progression through modulating the ErbB and Hippo pathways. Due to the crucial roles of miR-548c-3p in multiple types of cancer, development of novel gene therapies based on miR-548c-3p might be encouraged.

Taken together, the present study indicated that hsa_circ_0008287 and hsa_circ_0005027 were downregulated in HCa and competitively bound miR-548c-3p with ErbB and Hippo signaling pathway genes. Further studies are warranted on the roles of hsa_circ_0008287, hsa_circ_0005027, and miR-548c-3p as potential diagnostic biomarkers and therapeutic targets for HCa.

Acknowledgements

Not applicable.

Funding

This work was funded by Yunnan Applied Basic Research Projects (grant no. 2016FB038).

Availability of data and materials

The sequencing data have been deposited in the Gene Expression Omnibus (GEO) database under the accession number GSE111423.

Authors' contributions

CF designed experiments and helped analyze the data. YaL, YuL and XC collected the samples. DL analyzed data. HZ interpreted the results and wrote the manuscript. XH designed experiments and interpreted the results. All authors read and approved the final manuscript.

Ethics approval and consent to participate

The study was approved by the Ethics Committee of the First Affiliated Hospital of Kunming Medical University (Kunming, China). Written informed consent was obtained from all the participants in the study.

Patient consent for publication

Not applicable.

Competing interests

The authors declare that they have no competing interests.

References

1. Pingree TF, Davis RK, Reichman O and Derrick L: Treatment of hypopharyngeal carcinoma: A 10-year review of 1,362 cases. Laryngoscope 97: 901-904, 1987.
2. Chan JY and Wei WI: Current management strategy of hypopharyngeal carcinoma. Auris Nasus Larynx 40: 2-6, 2013.
3. Lagha A, Chraiet N, Labidi S, Rifi H, Ayadi M, Krimi S, Allani B, Raies H, Touati S and Boussen H: Larynx preservation: What is the best non-surgical strategy? Crit Rev Oncol Hematol 88: 447-458, 2013.
4. Carrasco Llatas M, Lopez Molla C, Balaguer Garcia R, Ferrer Ramírez MJ, Guallart Doménech F, Estellés Ferriol JE, Fernández Martínez S and Dalmau Galofre J: Hypopharyngeal cancer: Analysis of the evolution and treatment results. Acta Otorrinolaringol Esp 60: 3-8, 2009 (In Spanish).
5. Chen LL and Yang L: Regulation of circRNA biogenesis. RNA Biol 12: 381-388, 2015.
6. Memczak S, Jens M, Elefsinioti A, Torti F, Krueger J, Rybak A, Maier L, Mackowiak SD, Gregersen LH, Munschauer M, *et al*: Circular RNAs are a large class of animal RNAs with regulatory potency. Nature 495: 333-338, 2013.
7. Xie H, Ren X, Xin S, Lan X, Lu G, Lin Y, Yang S, Zeng Z, Liao W, Ding YQ and Liang L: Emerging roles of circRNA_001569 targeting miR-145 in the proliferation and invasion of colorectal cancer. Oncotarget 7: 26680-26691, 2016.
8. Zheng Q, Bao C, Guo W, Li S, Chen J, Chen B, Luo Y, Lyu D, Li Y, Shi G, *et al*: Circular RNA profiling reveals an abundant circHIPK3 that regulates cell growth by sponging multiple miRNAs. Nat Commun 7: 11215, 2016.
9. Guarnerio J, Bezzi M, Jeong JC, Paffenholz SV, Berry K, Naldini MM, Lo-Coco F, Tay Y, Beck AH and Pandolfi PP: Oncogenic role of fusion-circRNAs derived from cancer-associated chromosomal translocations. Cell 165: 289-302, 2016.
10. Zhong ZY, Lv MX and Chen JX: Screening differential circular RNA expression profiles reveals the regulatory role of circTCF25-miR-103a-3p/miR-107-CDK6 pathway in bladder carcinoma. Sci Rep 6: 30919, 2016.
11. Hansen TB, Jensen TI, Clausen BH, Bramsen JB, Finsen B, Damgaard CK and Kjems J: Natural RNA circles function as efficient microRNA sponges. Nature 495: 384-388, 2013.
12. Brown J, Pirrung M and McCue LA: FQC Dashboard: Integrates FastQC results into a web-based, interactive, and extensible FASTQ quality control tool. Bioinformatics 33: 3137-3139, 2017.
13. Gao Y, Wang J and Zhao F: CIRI: An efficient and unbiased algorithm for de novo circular RNA identification. Genome Biol 16: 4, 2015.
14. Li H and Durbin R: Fast and accurate short read alignment with Burrows-Wheeler transform. Bioinformatics 25: 1754-1760, 2009.
15. Harrow J, Frankish A, Gonzalez JM, Tapanari E, Diekhans M, Kokocinski F, Aken BL, Barrell D, Zadissa A, Searle S, *et al*: GENCODE: The reference human genome annotation for the ENCODE project. Genome Res 22: 1760-1774, 2012.
16. Kozomara A and Griffiths-Jones S: miRBase: Integrating microRNA annotation and deep-sequencing data. Nucleic Acids Res 39: D152-D157, 2011.
17. Lever J, Krzywinski M and Atman N: Points of Significance: principal component analysis. Nat Methods 14: 641-642, 2017. doi: 10.1038/nmeth.4346.
18. Hotelling H: Analysis of a complex of statistical variables into principal components. J Educ Psychol 24: 417-441, 1933.
19. Ginestet C: ggplot2: Elegant graphics for data analysis. J R Stat Soc Ser A 174: 245-245, 2011.
20. Harris T and Hardin JW: Exact Wilcoxon signed-rank and Wilcoxon Mann-Whitney ranksum tests. Stata J 13: 337-343, 2013.
21. Benjamini Y and Hochberg Y: Controlling the false discovery rate: A practical and powerful approach to multiple testing. J Roy Stat Soc B Met 57: 289-300, 1995.
22. Huang da W, Sherman BT and Lempicki RA: Systematic and integrative analysis of large gene lists using DAVID bioinformatics resources. Nat Protoc 4: 44-57, 2009.
23. Dudekulay DB, Panda AC, Grammatikakis I, De S, Abdelmohsen K and Gorospe M: CircInteractome: A web tool for exploring circular RNAs and their interacting proteins and microRNAs. RNA Biol 13: 34-42, 2016.
24. Casper J, Zweig AS, Villarreal C, Tyner C, Speir ML, Rosenbloom KR, Raney BJ, Lee CM, Lee BT, Karolchik D, *et al*: The UCSC genome browser database: 2018 update. Nucleic Acids Res 46: D762-D769, 2018.
25. Agarwal V, Bell GW, Nam JW and Bartel DP: Predicting effective microRNA target sites in mammalian mRNAs. Elife 4: 7554, 2015.
26. Vlachos IS, Zagganas K, Paraskevopoulou MD, Georgakilas G, Karagkouni D, Vergoulis T, Dalamagas T and Hatzigeorgiou AG: DIANA-miRPath v3.0: Deciphering microRNA function with experimental support. Nucleic Acids Res 43: W460-W466, 2015.
27. Shannon P, Markiel A, Ozier O, Baliga NS, Wang JT, Ramage D, Amin N, Schwikowski B and Ideker T: Cytoscape: A software environment for integrated models of biomolecular interaction networks. Genome Res 13: 2498-2504, 2003.
28. Livak KJ and Schmittgen TD: Analysis of relative gene expression data using real-time quantitative PCR and the 2(T)(-Delta Delta C) method. Methods 25: 402-408, 2001.
29. Cancer Genome Atlas Research Network, Analysis Working Group: Asan University, BC Cancer Agency, *et al*: Integrated genomic characterization of oesophageal carcinoma. Nature 541: 169-175, 2017.
30. Lancar R and Funck-Brentano C: Survival analysis example based on an event history model from a clinical trial in cardiology. Rev Epidemiol Sante Publique 47: 613-618, 1999 (In French).
31. Mantel N: Evaluation of survival data and two new rank order statistics arising in its consideration. Cancer Chemother Rep 50: 163-170, 1966.
32. R Development Core Team: R: A language and environment for statistical computing. Vienna, Austria: The R Foundation for Statistical Computing, 2011.
33. Guo JU, Agarwal V, Guo H and Bartel DP: Expanded identification and characterization of mammalian circular RNAs. Genome Biol 15: 409, 2014.
34. Glazar P, Papavasileiou P and Rajewsky N: circBase: A database for circular RNAs. RNA 20: 1666-1670, 2014.
35. Tay Y, Rinn J and Pandolfi PP: The multilayered complexity of ceRNA crosstalk and competition. Nature 505: 344-352, 2014.
36. Salmena L, Poliseno L, Tay Y, Kats L and Pandolfi PP: A ceRNA hypothesis: The rosetta stone of a hidden RNA language? Cell 146: 353-358, 2011.
37. Karreth FA and Pandolfi PP: ceRNA cross-talk in cancer: When ce-bling rivalries go awry. Cancer Discov 3: 1113-1121, 2013.
38. Rodrigo JP, González MV, Lazo PS, Ramos S, Coto E, Alvarez I, García LA and Suárez C: Genetic alterations in squamous cell carcinomas of the hypopharynx with correlations to clinicopathological features. Oral Oncol 38: 357-363, 2002.
39. Rodrigo JP, Ramos S, Lazo PS, Alvarez I and Suarez C: Amplification of ERBB oncogenes in squamous cell carcinomas of the head and neck. Eur J Cancer 32A: 2004-2010, 1996.

40. Otsu M, Hayashi Y, Amatsu M and Itoh H: Immunohistochemical study of p53, EGF, EGF-receptor, v-erb B and ras p21 in squamous cell carcinoma of hypopharynx. Kobe J Med Sci 40: 139-153, 1994.
41. Ma Y, Yang Y, Wang F, Wei Q and Qin H: Hippo-YAP signaling pathway: A new paradigm for cancer therapy. Int J Cancer 137: 2275-2286, 2015.
42. Santucci M, Vignudelli T, Ferrari S, Mor M, Scalvini L, Bolognesi ML, Uliassi E and Costi MP: The Hippo pathway and YAP/TAZ-TEAD protein-protein interaction as targets for regenerative medicine and cancer treatment. J Med Chem 58: 4857-4873, 2015.
43. Guo L and Teng L: YAP/TAZ for cancer therapy: Opportunities and challenges (Review). Int J Oncol 46: 1444-1452, 2015.
44. Liu AM, Xu MZ, Chen J, Poon RT and Luk JM: Targeting YAP and Hippo signaling pathway in liver cancer. Expert Opin Ther Targets 14: 855-868, 2010.
45. Saladi SV, Ross K, Karaayvaz M, Tata PR, Mou H, Rajagopal J, Ramaswamy S and Ellisen LW: ACTL6A Is Co-amplified with p63 in squamous cell carcinoma to drive YAP activation, regenerative proliferation, and poor prognosis. Cancer Cell 31: 35-49, 2017.
46. Shi Y, Qiu M, Wu Y and Hai L: MiR-548-3p functions as an anti-oncogenic regulator in breast cancer. Biomed Pharmacother 75: 111-116, 2015.
47. Rane JK, Scaravilli M, Ylipää A, Pellacani D, Mann VM, Simms MS, Nykter M, Collins AT, Visakorpi T and Maitland NJ: MicroRNA expression profile of primary prostate cancer stem cells as a source of biomarkers and therapeutic targets. Eur Urol 67: 7-10, 2015.